Pergamon

Bioorganic & Medicinal Chemistry 7 (1999) 177–185

BIOORGANIC & MEDICINAL CHEMISTRY

# Optimization of Hydrophobic Domains in Peptides That Undergo Transformation from α-Helix to β-Fibril

Yuta Takahashi, Akihiko Ueno and Hisakazu Mihara*

*Department of Bioengineering, Faculty of Bioscience and Biotechnology, Tokyo Institute of Technology, Yokohama 226-8501, Japan*

Received 14 April 1998; accepted 22 October 1998

**Abstract**—Recent studies on peptide fibrillogenesis by the de novo method as well as amyloidogenic proteins including prion proteins and Alzheimer's β-peptides have provided insights into the conformational changes, such as α-helix to β-structure, involved in folding and misfolding processes. We have found that an exposed hydrophobic nucleation domain at N-terminal causes a structural transition of a peptide from α-helix to β-fibril. It became clear that N-terminal acyl groups of particular lengths in a 2α-helix peptide caused the peptide to undergo an α-to-β transition. The peptide with the octanoyl group (C8-2α) showed the highest rate of transformation. The study of the designed peptides revealed that these α-to-β transitions were closely related to the initial α-helix conformation and its stability. Engineering peptides that undergo α-to-β transitions are attractive not only to the study of pathogenic proteins such as prion proteins, but also to the control of self-assembly of peptides, which will lead to the development of peptidyl self-assembling materials. 

## Introduction

A number of studies on disease-related proteins, such as those involved in Alzheimer's or the prion diseases have led to improvements in our understanding of protein misfolding and transformation.[1–17] The studies have pointed out common and possible mechanisms for the formation of protein amyloid fibrils. Environments and mutations that might destabilize the native structures of proteins and facilitate the formation of partially unfolded intermediates have been demonstrated to be possible causes of the fibril formation of proteins.[1–6] Such intermediates undergo peptide conformational transitions, which initiate protein aggregation and then fibril formation. Especially in the prion protein (PrP), a highly α-helical structure in the monomeric $PrP^{C}$ is transformed to a β-sheet conformation in aggregated protease-resistant $PrP^{Sc}$.[7–13] Similarly, β-amyloid peptides composed of 39–43 amino acid residues are also transformed to the amyloid form with a cross-β-sheet structure.[14–17] Although the mechanisms and intermediates of these amyloid formations have not yet been fully understood, it has been suggested that the aggregation process for the proteins from a less-β-structured monomer plays a key role in the conformational changes and the formation of amyloid with a higher β-sheet content.[3,4] In general, one cause of protein misfolding and transformation is thought to be the exposure of the hydrophobic region of proteins in an unstable form to water environments, and the formation of aggregates that follows.

On the other hand, similar α-to-β transitions also occur through the correct-folding pathway from intermediates to native forms in proteins with a non-hierarchical folding mechanism such as β-lactoglobulin.[18–21] Moreover, the same peptide sequence named 'chameleon' adapted an α-helix or a β-strand at the different position in the protein, the B1 domain of protein G (GB1).[22] The protein named 'Janus' was successfully designed from the β-sheet-dominant protein, GB1, to the α-helical protein, Rop, by changing no more than half the sequence.[23] These studies suggest that the key feature in the α–β transition is the conversion from short-range interactions between nearby amino acid residues stabilizing an α-helix structure to long-range interactions between secondary structures stabilizing a β-sheet structure.

A simplified model peptide designed by the de novo strategy can provide useful information for constructing and manipulating peptide conformation, and elucidating complex folding and misfolding mechanisms.[24–26] The design method often uses the amphiphilic nature of peptide secondary structures to construct tertiary structures of artificial proteins.[27] Peptides designed for β-sheet folding have been extensively studied,[28] and subsequent formation of fibrils has been characterized.[29] Model peptides homologous to parts of native proteins

Key words: Peptides and polypeptides; fibrillogenesis; α-helix; β-sheet; structural transition.

*Corresponding author: Tel: +81-45-924-5756; Fax: +81-45-924-5833; E-mail: hmihara@bio.titech.ac.jp

0968-0896/99/$ - see front matter 
*PII:* S0968-0896(98)00236-3

have been characterized as fibrillogenic peptides and their applications to molecular materials have been attempted.[30,31] Furthermore, some model peptides have been designed to allow α–β transitions via the replacement of environments from organic solvent to water,[32,33] the alteration of pH,[34,35] and the control of the redox state.[36,37] Therefore, these studies have revealed that control of the periodicity of hydrophobic and hydrophilic residues in a peptide sequence is essential in determining a secondary structure and α–β transitional properties. In other words, hydrophobic clustering between amphiphilic peptides seems to determine the secondary structures and their transformation.

We have also found that an exposed hydrophobic nucleation domain caused an α-to-β structural transition and fibril formation of a peptide.[3,38] The hydrophobic domain was designated as a hydrophobic defect, since it caused the aggregation and fibril formation of the peptide.[38] The first success of this approach for designing α-to-β transitional peptides was accomplished by using the adamantanecarbonyl (Ad) group as the N-terminal hydrophobic defect of the 2α-helix peptide. The Ad-linked 2α-peptide (Ad-2α) underwent an α-to-β transition and a β-fibril formation in an autocatalytic manner.[38] Using this strategy of adding hydrophobic defects of various acyl groups, in this study (Fig. 1), has revealed that the stability of the α-helix conformation in its initial state has a key role in determining whether or not the peptide structure will be transformed. The designed peptides mimicked an α-to-β transitional property of proteins such as prion proteins, a nucleation-dependent autocatalytic transformation.

## Results

### Peptide design and synthesis

A peptide composed of two amphiphilic α-helices[27] was designed, and acyl chains of various lengths were attached to the N-termini of the 2α-peptide as an exposed hydrophobic domain, i.e., as a hydrophobic defect (Fig. 1). The two-α-helix part was constructed from amino acid sequences of coiled-coil proteins, which had heptad repeats $(abcdefg)_n$ with hydrophobic residues at the a and d positions (Figure 1(B)).[39–41] The $<P_\alpha>$ and $<P_\beta>$ values of the core 14-peptide calculated with Chou–Fasman parameters[42] were 1.34 and 0.94, respectively. Therefore, judging only from the amino acid sequence the peptide was expected to form an α-helix structure. When the peptide sequence was drawn as a β-sheet model, the peptide could take a kind of amphiphilic β-sheet structure, in which hydrophobic Leu residues and hydrophilic Glu and Lys residues were separated on the different faces. The peptides were synthesized by the solid-phase method using 9-fluorenylmethyloxycarbonyl (Fmoc) chemistry.[43] The dimeric peptides (2α series) were synthesized via the disulfide linkage between Cys residues at the 17th position. The monomeric peptides (1α series) were used without the cleavage of the acetamidomethyl (Acm) protecting group.

### α-to-β Structural transition of 2α-peptides

The conformational changes of 2α-peptides with a variety of acyl chains (10 μM)[44] were examined by measuring circular dichroism (CD) spectra (Figure 2(A)). It was interesting that the α-to-β structural transition of peptides occurred optimally with octanoyl (C8) chain (Fig. 3). That is, the α-to-β transition of the 2α-peptide with octanoyl groups (C8-2α) occurred at the highest transitional rate among all of the peptides with acyl chains, the rate being almost identical to that of the adamantanecarbonyl peptide (Ad-2α) as the previous model.[38] C8-2α showed a CD spectrum typical for an α-helix structure ($[\theta]_{222} = -21{,}000$ deg·cm$^2$·dmol$^{-1}$) shortly after dilution in a buffer (pH 7.4) from the trifluoroethanol (TFE) solution (Figure 2(A)). The CD measurements revealed a gradual change in a spectrum typical for a β-structure, with a single minimum at

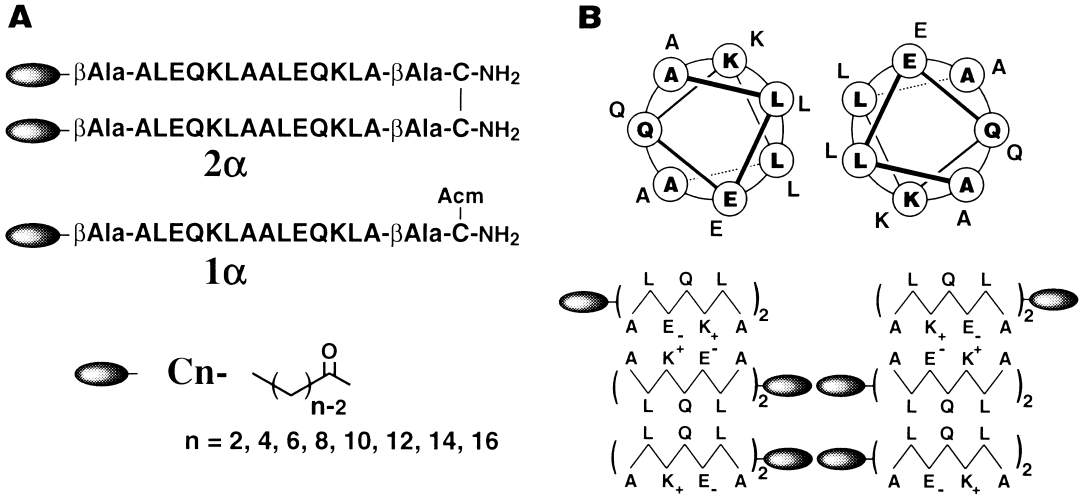


**Figure 1.** Structure of the 2α- and 1α-peptides with a variety of acyl chains as hydrophobic defects. (**A**) Amino acid sequences of the peptides, 2α and 1α, with a hydrophobic defect of aliphatic acyl chains (Cn-). (**B**) Helix wheel drawing as a coiled-coil form and illustation of associated β-structures of the core 14-peptide in 2α-peptides.

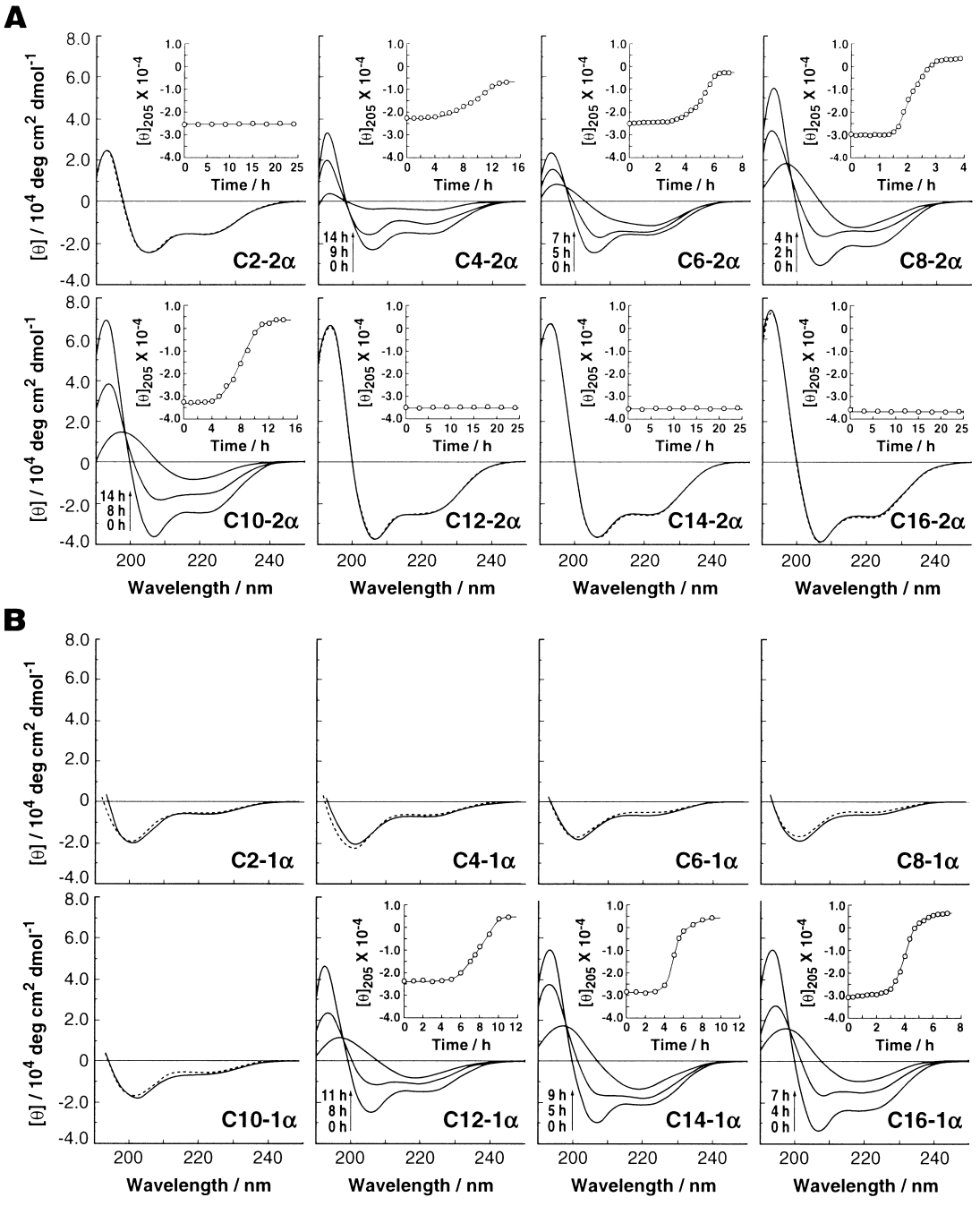


**Figure 2.** CD studies of the Cn-peptides. Spectral changes and time courses (inset) of ellipticity change at 205 nm of Cn-2α (**A**) and Cn-1α (**B**). The TFE solution of Cn-peptides was diluted in 20 mM Tris·HCl (pH 7.4) (final TFE content;2.5%) and the CD spectra were measured at several intervals. The broken line denotes the spectrum after 1 day. [peptide] = 10 μM (Cn-2α) and 20 μM (Cn-1α) at 25 °C.

218 nm ($[\theta]_{218} = -14{,}000$ deg·cm$^2$·dmol$^{-1}$) and a maximum at 198 nm after 4 h at 25 °C (half transition time $t_{1/2} = 120$ min). The time course of the structural transition was quite sigmoidal, resembling the autocatalytic transition process in β-amyloid and prion peptides.[14,45–50]

Transmission electron micrograph showed that C8-2α which was in the β-structure formed amyloid fibrils in ca. 10 nm width with a morphology similar to that of Alzheimer's β-peptides or prion proteins (Fig. 4).[51,52] Furthermore, the fibrils assembled into larger deposits (10–100 μm size) stained by Congo red[53] or thioflavin T.[54] Observation of deposits by microscopy in the presence of thioflavin T revealed that the fibril formation of the peptides occurred coincidentally with the α-to-β transitions.[38]

On the other hand, the CD spectra of C2-2α did not show a transition to a β-structure, but remained in α-helix. The CD spectra of C4- and C6-2α changed over 14 and 7 h, respectively, but their shapes indicated the presence of a mixture of α-helix and β-sheet, with the content of β-structure of C6-2α being higher than that of C4-2α. As the chain length increased, the α-to-β

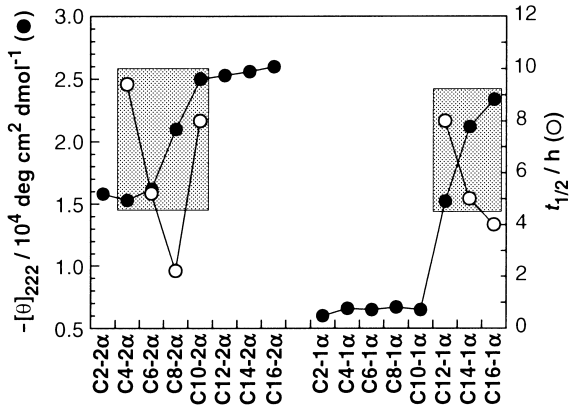


**Figure 3.** Plots of the ellipticity at 222 nm at 0 h (●) and the half transition time $t_{1/2}$ detected by $[\theta]_{205}$ (○) of Cn-peptides. Ellipticities for the transitional peptides are highlighted with shaded squares.

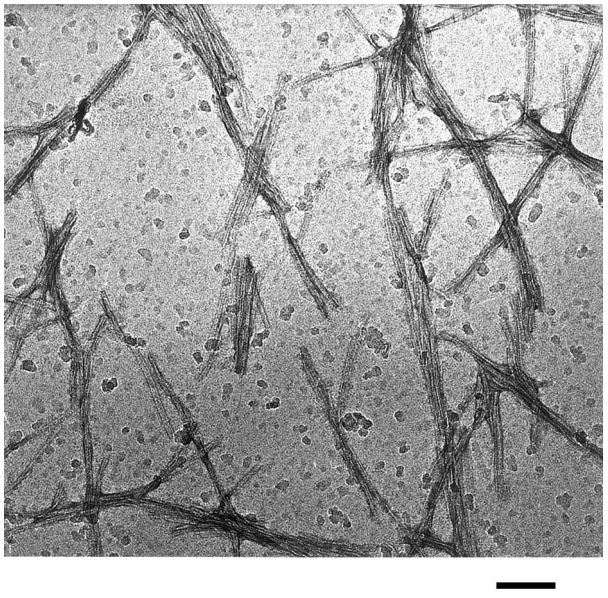

**Figure 4.** Electron micrograph of C8-2α in the β-structure. The aggregates were formed by incubating 10 μM C8-2α in 20 mM Tris·HCl buffer (pH 7.4) with 2.5% TFE at 25 °C for 8 h, and then negatively strained with a 2% aqueous uranyl acetate on the grid. Magnification, 25000×; scale bar 100 nm.

transition appeared to take place more rapidly and completely. The peptides with C8 and C10 showed an almost complete α-to-β transition, though the rate of transition for C10-2α was lower than that of C8-2α. In contrast, the peptides with acyl chains longer than C10 (C12- to C16-2α) formed α-helix, but showed no sign of making an α-to-β transition. These results indicated that the hydrophobic defect was important for the 2α-helix peptide to transform to β-structure, but there was an optimum in the hydrophobicity of the defect. Whether or not the peptides are able to make the α-to-β transition appears to be related to the peptide ellipticity in the initial α-helix state. Peptides with longer acyl chains showed a larger ellipticity at 222 nm (Fig. 3). The longer acyl chains provided a higher degree of stabilization for the α-helix structure in its initial state.

## α-to-β Structural transition of 1α-peptides

The conformations and structural transitions of 1α-peptides (20 μM) were also examined (Figure 2(B)). The 1α-peptides with acyl chains longer than C10 (C12- to C16-1α) showed α-helical CD spectra in their initial state, but these appeared to change to the spectra of β-structures after 6–12 h. In contrast, corresponding 2α-peptides were highly α-helical, but not transformed. On the other hand, the 1α-peptides with chains shorter than C12 (C2- to C10-1α) showed CD spectra indicating an almost random structure, and the conformations of these peptides were not transformed. Whether or not the 1α-peptide takes on an α-helix structure in its initial state appears to determine its ability to make the α-to-β structural transition. It is worth noting that ellipticities of the 1α-peptides (C12- to C16-1α) were in the range of those of the 2α-peptides (C4- to C10-2α) that underwent the α-to-β transition (Fig. 3).

## Size-exclusion chromatography

Size-exclusion chromatography revealed that the apparent molecular weight (MW) of the peptides, estimated using the protein standards, correlated to their α-helix propensities and their α-to-β transitional properties (Fig. 5). The peptides in TFE were injected into a Superdex 75 HR equilibrated with 50 mM phosphate buffer (pH 7.0). The retention time of the peptides could reflect their apparent MW at almost the initial state. The observed MW of the 2α-peptides gradually decreased for the chain length up to C8. C8-2α showed a minimum value in the apparent MW, which closely corresponded to the theoretical MW. At chain lengths longer than C8, however, the apparent MW of the 2α-peptides increased dramatically. As shown in the CD studies (Figs 2(A) and 3), peptides with a shorter chain showed a lower α-helicity, meaning that the shorter acyl peptides had a more extended structure. Therefore, it is reasonable to assume that the peptides with a chain length shorter than C10 (C2- to C8-2α) are in a monomer form at the initial state, although the apparent MW of the peptides with shorter chain lengths was slightly larger (1.0–1.7 times) than the expected MW. Interestingly, the peptides with longer acyl chains (C10- to C16-2α) formed stable oligomers in α-helix. The MW of the oligomers became higher as the chain length increased. According to the protein standards, C10-, C12-, C14-, and C16-2α formed 2.6, 2.9, 3.0, and 3.3 mer, respectively. The 2α-peptides forming stable α-helix oligomers did not possess the α-to-β transitional property, whereas the α-to-β transitional peptides seemed to be monomeric in the initial α-helix state with the exception of C10-2α. The elution shape of C10-2α was broadened as compared with those of other monomeric and oligomeric peptides, indicating that the oligomeric state of C10-2α was more unstable than those of the peptides with longer acyl chains.

In the 1α-peptides, the peptides with acyl chains longer than C10 (C12- to C16-1α) appeared to be in an α-helix structure at the initial state and could not be detected by size-exclusion chromatography, suggesting that these

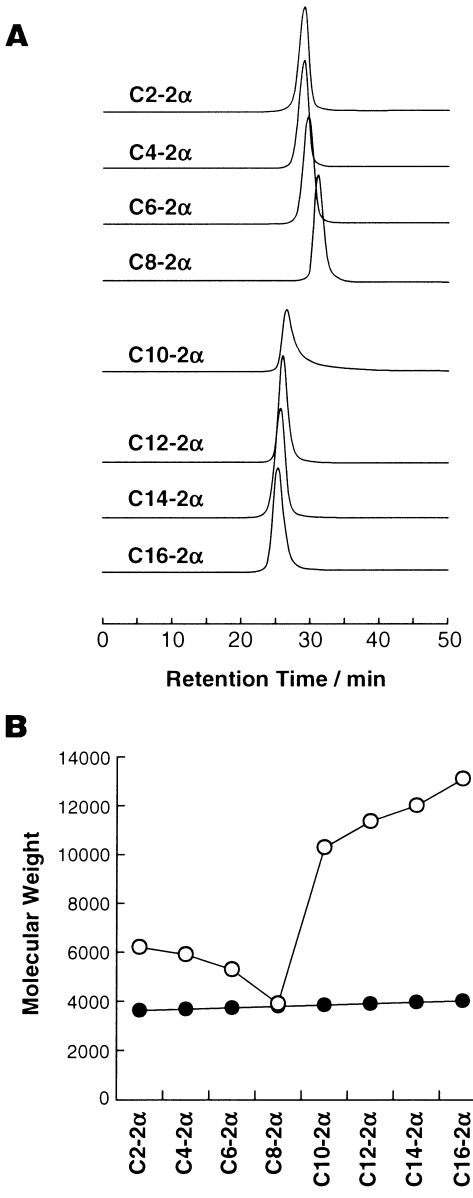


**Figure 5.** Size-exclusion chromatography of Cn-2α in α-form. (**A**) size-exclusion chromatograms of Cn-2α. (**B**) Plots of the apparent MW (○) according to protein standards and the theoretical MW (●). Column, Superdex 75 HR 10/30; eluent, 50 mM phosphate buffer (pH 7.0); detection, 220 nm; [injected peptide] = 0.4 mM in TFE at 25 °C.

peptides formed multiple and/or higher levels of aggregates that prevented their detection even in the initial state. The random structure 1α-peptides with shorter chains (C2- to C10-1α), were considered to be monomeric according to the elution times (data not shown).

## Denaturation experiments

The CD and gel-filtration studies suggested that the α-helix stability and formation of α-helix oligomers were related to whether or not the peptides underwent the α-to-β transition. The stability of α-helices was examined by denaturation experiments using guanidine hydrochloride (GuHCl) (Fig. 6).[55] Shortly after dilution from the TFE solution, the α-forms of C2- to C8-2α were completely unfolded in the presence of 4 M GuHCl. The

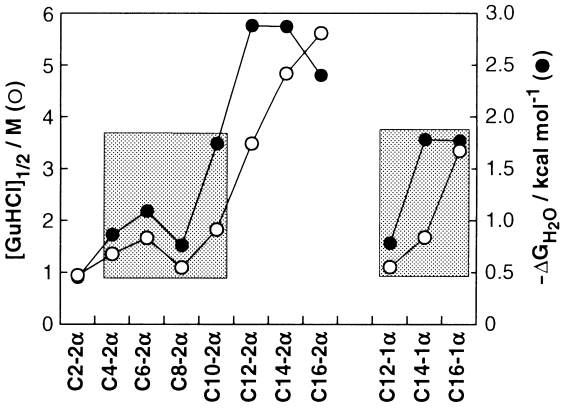


**Figure 6.** Denaturation experiments of Cn-2α and Cn-1α in α-forms using guanidine hydrochloride (GuHCl). Plots of the half denaturation concentration of GuHCl, $[GuHCl]_{1/2}$, (○) and the stability, $-\Delta G_{H_2O}$, (●). [peptide] = 10 μM (Cn-2α) and 20 μM (Cn-1α) at 25 °C. The plots for the transitional peptides are highlighted with shaded squares.

denaturation curves of C2- to C8-2α showed the half-denaturation concentration $[GuHCl]_{1/2} = 0.9$ to 1.7 M, the stability $\Delta G_{H_2O} = -0.5$ to $-1.1$ kcal mol$^{-1}$, indicating that the α-helix conformations of these peptides were not very stable, unlike other peptides designed by the de novo method.[24] In contrast, the α-helix stability increased dramatically as the chain lengthened for peptides longer than C8. The α-forms of C12- to C16-2α, which were in α-helix oligomers, showed higher stabilities in GuHCl ($[GuHCl]_{1/2} = 3.5$ to 5.6 M, $\Delta G_{H_2O} = -2.4$ to $-2.9$ kcal mol$^{-1}$). The curve profile of $[GuHCl]_{1/2}$ and $\Delta G_{H_2O}$ values against the chain length resembled those seen in ellipticity (Fig. 3) and size-exclusion chromatography (Fig. 5), suggesting that the α-helix stability was reflected by the α-helix oligomerization. It is interesting that C8-2α, the fastest-transitional peptide, showed minimum values in $[GuHCl]_{1/2}$ and $\Delta G_{H_2O}$ among the Cn-2α peptides (C4- to C10-2α) that underwent the structural transitions. A likely reason for this is that C8-2α folds less cooperatively than other peptides, probably due to a higher degree of solvent exposure in the interior or the acyl group,[56] which might accelerate the α-to-β structural transition.

In the case of 1α-peptides C12-, C14-, and C16-1α, increases in chain length led to a higher stability of peptides against the denaturant (Fig. 6). The Cn-1α peptides, however, showed larger transitional rates as the chain lengths increased. Furthermore, the stability of 1α-helix peptide was lower than that of the corresponding 2α-helix peptide, suggesting that the initial α-helix states of 1α-helix and 2α-helix peptides were different, as indicated by the size-exclusion chromatography experiments. It should be noted that the stabilities of 1α-helix peptides were in the range of the stabilities of 2α-helix peptides (C4- to C10-2α) that underwent the α-to-β transition.

## Effect of detergents

A cationic detergent, cetyltrimethylammonium bromide (CTAB), and an anionic detergent, sodium dodecylsulfate (SDS), inhibited the structural transition of

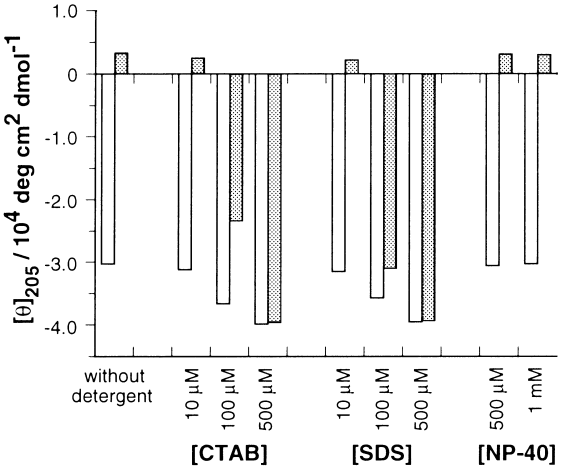


**Figure 7.** Effects of various detergents on the α-β transition of C8-2α. Open and shaded bars denote $[\theta]_{205}$ at 0 h and 24 h, respectively. CTAB, cetytrimethylammonium bromide; SDS, sodium dodecylsulfate; NP-40, nonylphenoxy polyethoxyethanol. [peptide] = 10 μM at 25 °C.

C8-2α in a concentration-dependent manner (Fig. 7). Both detergents completely inhibited the α-to-β transition at concentrations over 500 μM. The transition was retarded at the detergent concentrations under 500 μM. The detergents could be expected to affect the hydrophobic interactions between the C8 groups and between helices, resulting in perturbation of 3-D structure and separation of the two α-helices, allowing each helix to move independently. The fact that the addition of TFE in more than 5% solvent content completely prevented the transition supported the assumption that the hydrophobic interactions were important (data not shown).[38] When the detergents were added, the α-helicity of C8-2α at the initial state (open columns in Figure 7) was increased depending on the amount of the detergents, meaning that the increase in α-helical content of the peptide was also responsible for retardation of the α-to-β transition. However, the dominant factor in preventing or retarding the transition by detergents or TFE appeared not to be the increase in the helical content but the reduction of hydrophobic intermolecular interaction, since the increased helical content did not always inhibit the transition as shown in the results of C4- to C8-2α, or C12- to C16-1α (Fig. 3). It is worth noting that some cationic detergents were reported to be inhibitors of the fibril formation of β-amyloid peptide.[57] The non-ionic detergent NP-40 did not inhibit the structural transition up to 5 mM. Perturbation of electrostatic interactions as well as the hydrophobic interactions by the cationic and anionic detergents might be effective at inhibiting the reaction.

## Discussion

We have demonstrated that if Ad-group was added to a 2α-helix peptide as an exposed hydrophobic domain, an α-to-β structural transition was triggered after a lag time.[38] The transitional profile appeared to be nucleation-dependent and autocatalytic. C2-2α without the hydrophobic defect and Ad-linked 1α-peptide in a random structure were not transformed to a β-structure. To explore the effect of the hydrophobicity of the conformational defects, we newly synthesized monomeric 1α- and dimeric 2α-peptides with a variety of acyl chains and examined the conformational properties. Among the acyl-chained 2α-peptides ranging from C2 to C16, the octanoyl group was the most effective for inducing the α-to-β transition under the conditions of μM level. Using the octanoyl group provided optimum hydrophobicity for the conformational defects. The peptides with lower hydrophobicity than C6 showed a lower α-helix propensity, but did not completely transform to a β-structure. The peptides with higher hydrophobicity than C10 (C12- to C16-2α) formed stable α-helix oligomers, but did not transform to a β-structure. The 2α-peptides with longer acyl chains (C12- to C16-2α) formed more stable α-helices than C8-2α due to the formation of oligomers in the initial α-helix state. The transitional peptides (C4- to C8-2α) were in a monomeric state at the initial stage. Among 1α-peptides, those capable of forming an α-helix also had the transitional property. The α-to-β transition was closely related to the α-helix conformation and its moderate stability in its initial state.

This study using the acyl chains, in addition to the previous work with Ad-group,[38] suggest that unstable α-helix aggregates (oligomer or larger) are an intermediate (nucleus) of the structural transition (Fig. 8). Based on this assumption, the conformation of a peptide with moderate hydrophobicity, such as that of Ad-2α or C8-2α, would exist in equilibrium between a monomer and aggregates in α-helix. When a critical amount of α-helix aggregates accumulate, which gives rise to new long-range (intermolecular) interactions, the peptide conformation transforms to β-sheet in an autocatalytic manner. The time necessary for the accumulation of

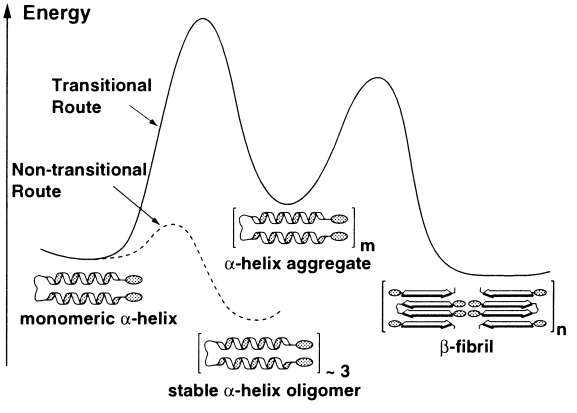


**Figure 8.** A proposed mechanism of the α-to-β transition. Formation and instability of the α-helix aggregates as an intermediate are key features of the α-to-β transition. The conformation of a peptide with moderate hydrophobicity, such as that of C8-2α, would exist in an equilbrium between a monomer and aggregates in α-helix. The time necessary for the accumulation of α-helix aggregates may correspond to the lag time for nucleation.[38] When a critical amount of α-helix aggregates accumulate, which gives rise to new long-range (intermolecular) interactions, the conformational change to β-sheet occurs cooperatively. On the contary, peptides with the longer acyl chain such as C16 form more stable α-helix oligomers and could not further assemble into larger aggregates, thus could not transform to a β-sheet structure.

α-helix aggregates may correspond to the lag time for nucleation,[38] although the α-helix aggregates are so unstable that they cannot be detected by the size-exclusion method. Once the β-aggregates appear, monomeric or oligomeric α-helix species could further transform to the β-sheet on the template aggregates. In contrast, when a peptide forms stable α-helix oligomers such as C12- to C16-2α, the conformation of the peptide is not transformed. A peptide with a less hydrophobic domain, such as C2-2α, remains stable as a monomeric 2α-helix and cannot form an α-helix nucleus, thus cannot acquire the long-range interaction that would stabilize the β-structure. Therefore, there appears to be an optimum length for the hydrophobic defects.

One role of the hydrophobic defects would thus be the formation of an α-helix nucleus. In other words, the hydrophobic clustering by the conformational defects may form unstable α-helix aggregates, which would then initiate the cooperative conversion from short-range interactions to long-range interactions, thereby triggering the autocatalytic transition to β-sheet conformation. The two-segmental peptide is designed to form either an amphiphilic α-helix or an amphiphilic β-sheet using Leu residues for the hydrophobic core (Fig. 1), indicating that it may be a chameleon.[22] In fact, there is only a marginal difference (~1 kcal $mol^{-1}$) between the free energies of stabilization of the α and β conformations of Ad-2α model.[38] The conformation of such a de novo designed peptide has been characterized as a molten-globule-like structure.[24,25] Although the mechanism of the α-to-β transition step is certainly more complex and will require further clarification, it is plausible that the formation of unstable α-helix aggregates like a molten-globule-like structure occurs during the lag time and is the rate-determining step and, therefore, that the initial α-helix structure and its stability are significant determinants for the transition. It has also been suggested that the formation of relatively unstable intermediates of proteins in folding pathways or by unfavorable mutations triggers the aggregation and structural transition.[4,58,59] Especially in the prion proteins, it has been proposed that the transformation from an α-helix to a β-sheet structure induces the formation of aggregates as a seed for amyloidogenesis.[17,60,61] The initiation of α-to-β transition by introducing hydrophobic domains may provide insight into the conformational changing process that has been widely observed in protein research. The design concept employed here could potentially lead to a model system for clarifying off-pathway aggregations of proteins as well as for controlling self-assembly of polypeptides, which will also lead to the development of peptidyl self-assembling materials.[30,31]

## Experimental

### General methods

All chemicals and solvents were of reagent or HPLC grade. Amino acid derivatives and reagents for peptide synthesis were purchased from Watanabe Chemical Co. (Hiroshima, Japan). All peptides were synthesized by the solid phase method using Fmoc chemistry.[43] The peptides were purified by reversed-phase HPLC (RP-HPLC) on a YMC-Pack C4 A-823 column (10×250 mm) (YMC Co.) using a linear gradient at a flow rate of 3.0 mL $min^{-1}$. HPLC was performed on Hitachi L-7000 instruments. The peptides were identified by matrix assisted laser desorption ionization time-of-flight mass spectrometry (MALDI-TOFMS) and amino acid analysis. MALDI-TOFMS were performed on a Shimadzu KOMPACT MALDI III mass spectrometer using 3,5-dimethoxy-4-hydroxycinnamic acid as a matrix. Amino acid analyses were carried out on a JEOL JLC-300 system with ninhydrin detection after hydrolysis in 6 M HCl at 110 °C for 24 h in a sealed tube.

### Peptide synthesis

1α-Peptides. Fmoc-βAla-Ala-Leu-Glu(O*t*Bu)-Gln(Trt)-Lys(Boc)-Leu-Ala-Ala-Leu-Glu(O*t*Bu)-Gln(Trt)-Lys-(Boc)-Leu-Ala-βAla-Cys(Acm)-Rink amide resin (*t*Bu, *tert*-butyl; Trt, trityl; Boc, *tert*-butyloxycarbonyl; Acm, acetamidomethyl) was synthesized by stepwise elongation of Fmoc-amino acids (3 equiv) on 4-(2′,4′-dimethoxyphenyl-aminomethyl)phenoxy resin (Rink amide resin)[62] using benzotriazol-1-yloxytris(dimethylamino)-phosphonium hexafluorophosphate (BOP)[63] (3 equiv) as a coupling reagent and 20% piperidine/*N*-methylpyrrolidone for deprotection. To introduce acyl groups, acetic anhydride or $CH_3(CH_2)_nCOCl$ ($n=2$–14) (10 equiv) was used. The peptides with the Acm group were cleaved from the resin by the treatment with TFA (10 mL) in the presence of *m*-cresol (0.25 mL) and thioanisole (0.75 mL) for 60 min at room temperature. The 1α-peptides were purified by RP-HPLC to give a single peak on an analytical RP-HPLC, and characterized by MALDI-TOFMS and amino acid analysis: MALDI-TOFMS found $M+H^+$ (calcd $M+H^+$); C2-1α, 1884.7 (1884.2); C4-1α, 1912.7 (1912.3); C6-1α, 1940.5 (1940.3); C8-1α, 1968.4 (1968.4); C10-1α, 1996.3 (1996.5); C12-1α, 2024.2 (2024.5); C14-1α, 2052.8 (2052.6); C16-1α, 2079.8 (2079.3).

2α-Peptides. To remove the Acm group of 1α-peptides, the peptides were treated with $AgBF_4$ (20 equiv) in the presence of anisole (10 equiv) in TFA (2 mL) at 0 °C for 60 min.[64] The solvent was evaporated and the peptide-Ag salt was precipitated with diethylether. The precipitates were collected by centrifugation and dried with argon gas. The powder was dissolved in dimethylsulfoxide (DMSO) and then 1 M HCl was added (50% DMSO/1 M HCl) to form the disulfide linkage.[65] The solution was stirred at room temperature for 1 day to give the 2α-peptides. The solution was centrifuged to remove AgCl and then the products were purified by RP-HPLC. The peptides were characterized by MALDI-TOFMS and amino acid analysis: MALDI-TOFMS found $M+H^+$ (calcd $M+H^+$); C2-2α, 3624.0 (3623.3); C4-2α, 3680.0 (3679.4); C6-2α, 3735.7 (3735.4); C8-2α, 3792.5 (3791.6); C10-2α, 3847.9 (3847.7); C12-2α, 3903.8 (3903.8); C14-2α, 3960.4 (3959.9); C16-2α, 4015.8 (4016.0).

### Circular dichroism measurements

CD measurements were performed on a Jasco J-720WI spectropolarimeter equipped with a thermo-regulator using a quartz cell with 1.0-mm pathlength. Spectra were recorded in terms of mean residue ellipticity ([θ], in deg·cm$^2$·dmol$^{-1}$). Stock solution of each peptide in TFE was diluted in 20 mM Tris·HCl buffer (pH 7.4). Final concentrations of 1α- and 2α-peptides were 20 μM and 10 μM, respectively, and TFE content was 2.5%.

GuHCl denaturation studies were carried out by preparing the peptide solution in the buffer containing GuHCl and 2.5% TFE from the peptide stock solution. For the denaturation of the peptides in α-form, measurements were done shortly after the dilution from the stock solution in TFE. The denaturation curves were fitted to the equation $\Delta G_{obs} = \Delta G_{H_2O} - m[GuHCl]$, where $\Delta G_{obs} = -RT\ln((1-f)/f)$ ($f$ is the fraction of folded peptide), $\Delta G_{H_2O}$ is the free energy of folding in the absence of denaturant, and $m$ is the change in the molar cosolvation free energy.[55]

### Transmission electron microscopy

Peptide solution was prepared and incubated as described in the CD measurements (10 μM peptide in 20 μM Tris·HCl buffer (pH 7.4) with 2.5% TFE at 25 °C). The sample was absorbed to a carbon-coated copper grid (200 mesh) by floating the grid on a drop of the peptide solution for 30 s. The excess solution was removed by filter paper blotting and the grid was washed by floating on a drop of water for 10 s and then the water was removed. The sample on the grid was then negatively stained with a 2% (w/v) aqueous uranyl acetate for 30 s and the excess staining solution was removed. After drying, the samples were visualized with a JEOL 1200EX electron microscope operating at 80 kV.

### Size-exclusion chromatography

For analytical size-exclusion HPLC, a Superdex 75 HR column (10×300 mm) (Pharmacia Biotech) was used with 50 mM phosphate buffer (pH 7.0) as an eluent at a flow rate of 0.5 mL min$^{-1}$. Following proteins were used as molecular weight standards: albumin (66000), carbonic anhydrase (29000), cytochrome *c* (12400), aprotinin (6500), and insulin B chain (3500).

## Acknowledgements

This work was supported in part by a Grant-in-Aid for Scientific Research from the Ministry of Education, Science, Culture and Sports, Japan, and by a research grant from the Ogasawara Foundation for the Promotion of Science and Engineering.

## References and Notes

1. Taubes, G. *Science* **1996**, *271*, 1492.
2. Wetzel, R. *Cell* **1996**, *86*, 699.
3. Mihara, H.; Takahashi, Y. *Curr. Opin. Struct. Biol.* **1997**, *7*, 501.
4. Kelly, J. W. *Curr. Opin. Struct. Biol.* **1996**, *6*, 11.
5. Speed, M. A.; Wang, D. I. C.; King, J. *Nature Biotech.* **1996**, *14*, 1283.
6. Bychkova, V. E.; Ptitsyn, O. B. *FEBS Lett.* **1995** *359*, 6.
7. Prusiner, S. B. *Science* **1991**, *252*, 1515.
8. Prusiner, S. B. *Science* **1997**, *278*, 245.
9. Harrison, P. M.; Bamborough, P.; Daggett, V.; Prusiner, S. B.; Cohen, F. E. *Curr. Opin. Struct. Biol.* **1997**, *7*, 53.
10. Riek, R.; Hornemann, S.; Wider, G.; Billeter, M.; Glockshuber, R.; Wüthrich, K. *Nature* **1996**, *382*, 180.
11. Riek, R.; Hornemann, S.; Wider, G.; Glockshuber, R.; Wüthrich, K. *FEBS Lett.* **1997**, *413*, 282.
12. Korth, C.; Stierli, B.; Streit, P.; Moser, M.; Schaller, O.; Fischer, R.; Schulz-Schaeffer, W.; Kretzschmar, H.; Glockshuber, R.; Riek, R.; Billeter, M.; Wüthrich, K.; Oesch, B. *Nature* **1997**, *390*, 74.
13. Peretz, D.; Williamson, R. A.; Matsunaga, Y.; Serban, H.; Pinilla, C.; Bastidas, R. B.; Rozenshteyn, R.; James, T. L.; Houghten, R. A.; Cohen, F. E.; Prusiner, S. B.; Burton, D. R. *J. Mol. Biol.* **1997**, *273*, 614.
14. Lansbury, Jr. P. T. *Acc. Chem. Res.* **1996**, *29*, 317.
15. Selkoe, D. J. *J. Biol. Chem.* **1996**, *271*, 18295.
16. Forloni, G.; Tagliavini, F.; Bugiani, O.; Salmona, M. *Prog. Neurobiol.* **1996**, *49*, 287.
17. Kelly, J. W.; Lansbury, Jr. P. T. *Amyloid: Int. J. Exp. Clin. Invest.* **1994**, *1*, 186.
18. Hamada, D.; Segawa, S.; Goto, Y. *Nature Struct. Biol.* **1996**, *3*, 868.
19. Kuroda, Y.; Hamada, D.; Tanaka, T.; Goto, Y. *Folding Des.* **1996**, *1*, 255.
20. Hamada, D.; Kuroda, Y.; Tanaka, T.; Goto, Y. *J. Mol. Biol.* **1995**, *254*, 737.
21. Kuwajima, K.; Yamaya, H.; Sugai, S. *J. Mol. Biol.* **1996**, *264*, 806.
22. Minor, Jr. D. L.; Kim, P. S. *Nature* **1996**, *380*, 730.
23. Dalal, S.; Balasubramanian, S.; Regan, L. *Nature Struct. Biol.* **1997**, *4*, 548.
24. Betz, S. F.; Raleigh, D. P.; DeGrado, W. F. *Curr. Opin. Struct. Biol.* **1993**, *3*, 601.
25. Betz, S. F.; Bryson, J. W.; DeGrado, W. F. *Curr. Opin. Struct. Biol.* **1995**, *5*, 457.
26. Hill, R. B.; DeGrado, W. F. *J. Am. Chem. Soc.* **1998**, *120*, 1138.
27. Kaiser, E. T.; Kézdy, F. J. *Science* **1984**, *223*, 249.
28. Schneider, J. P.; Kelly, J. W. *Chem. Rev.* **1995**, *95*, 2169.
29. Choo, D. W.; Schneider, J. P.; Graciani, N. R.; Kelly, J. W. *Macromolecules* **1996**, *29*, 355.
30. Aggeli, A.; Bell, M.; Boden, N.; Keen, J. N.; Knowles, P. F.; McLeish, T. C. B.; Pitkeathly, M.; Radford; S. E. *Nature* **1997**, *386*, 259.
31. Zhang, S.; Rich, A. *Proc. Natl. Acad. Sci. USA* **1997**, *94*, 23.
32. Mutter, M.; Hersperger, R. *Angew. Chem., Int. Ed. Engl.* **1990**, *29*, 185.
33. Ono, S.; Kameda, N.; Yoshimura, T.; Shimasaki, C.; Tsukuromichi, E.; Mihara, H.; Nishino, N. *Chem. Lett.* **1995**, 965.
34. Mutter, M.; Gassmann, R.; Buttkus, U.; Altmann, K.-H. *Angew Chem., Int. Ed. Engl.* **1991**, *30*, 1514.
35. Cerpa, R.; Cohen, F. E.; Kuntz; I. D. *Folding Des.* **1996**, *1*, 91.
36. Dado, G. P.; Gellman, S. H. *J. Am. Chem. Soc.* **1993**, *115*, 12609.
37. Schenck, H. L.; Dado, G. P.; Gellman, S. H. *J. Am. Chem. Soc.* **1996**, *118*, 12487.
38. Takahashi, Y.; Ueno; A.; Mihara, H. *Chem. Eur. J.* **1998**, *4*, 2475.
39. Kohn, W. D.; Kay, C. M.; Sykes, B. D.; Hodges, R. S. *J. Am. Chem. Soc.* **1998**, *120*, 1124.

40. O'Shea, E. K.; Klemm, J. D.; Kim, P. S.; Alber, T. *Science* **1991**, *254*, 539.
41. Sakamoto, S.; Sakurai, S.; Ueno, A.; Mihara, H. *Chem. Commun*. **1997**, 1221.
42. Chou, P. Y.; Fasman, G. D. *Biochemistry* **1974**, *13*, 222.
43. Atherton, E.; Sheppard, R. C. *Solid Phase Peptide Synthesis: A Practical Approach*; IRL Press: Oxford, 1989.
44. In the previous studies,[38] the concentration dependence of the transition of Ad-2α was investigated. Increases of peptide concentration of up to 10 μM linearly enhanced the reaction rate (slope) while shortening the lag time period for β-sheet formation. However, further increasing the concentration to more than 20 μM prevented the CD measurements due to the formation of insoluble materials. Under 10 μM concentration, no visible precipitate was observed. Thus, 10 μM concentration was selected as a standard condition.
45. Jarrett, J. T.; Lansbury, Jr. P. T. *Cell* **1993**, *73*, 1055.
46. Come, J. H.; Lansbury, Jr. P. T. *J. Am. Chem. Soc*. **1994**, *116*, 4109.
47. Watzky, M. A.; Finke, R. G. *J. Am. Chem. Soc*. **1997**, *119*, 10382.
48. Laurent, M. *FEBS Lett*. **1997**, *407*, 1.
49. Eigen, M. *Biophys. Chem*. **1996**, *63*, A1.
50. The α-to-β transition reaction of C8-2α was analyzed using schemes 1 and 2 for a simplest autocatalytic reaction,[47] where A-form converts to B-form by the non-catalytic first step with the rate constant $k_1$ and the self-catalytic second step with the rate constant $k_2$.

$$A \xrightarrow{k_1} B \quad (1)$$

$$A + B \xrightarrow{k_2} 2B \quad (2)$$

In this model, A is defined as species in α-helix and B is species in β-strand. From the Schemes 1 and 2, the evolution of B over time is described by the equation 3.

$$d[B]/dt = k_1[A] + k_2[A][B] \quad (3)$$

The α-to-β transition followed by CD spectral changes was well fitted to the equation based on this mechanism. The curve fitting analysis gave the rate constants of $k_1$: $5.2\times10^{-7}\,s^{-1}$ and $k_2$: $99\,M^{-1}\,s^{-1}$. According to this mechanism, the second self-catalytic step is 2000 times faster than the first non-catalytic step under the conditions ([peptide] = 10 μM). This analysis suggests that the transitional reaction possibly proceeds via the first self-transitional and the second self-catalytic steps, in which there is a kinetic barrier at the first step. Although the aggregation numbers were not considered in this analysis, the first self-transitional step may include the aggregation of α-helix peptides. The temperature dependence of Ad-2α[38] also suggested that the reaction occurring during the lag time was the rate-determining step and the rapid conformational transition followed.
51. Wood, S. J.; Maleeff, B.; Hart, T.; Wetzel, R. *J. Mol. Biol*. **1996**, *256*, 870.
52. Nguyen, J. T.; Inouye, H.; Baldwin, M. A.; Fletterick, R. J.; Cohen, F. E.; Prusiner, S. B.; Kirschner, D. A. *J. Mol. Biol*. **1995**, *252*, 412.
53. Klunk, W. E.; Pettegrew, J. W.; Abraham, D. J. *J. Histochem. Cytochem*. **1989**, *37*, 1273.
54. LeVine, III. H. *Protein Sci*. **1993**, *2*, 404.
55. Santoro, M. M.; Bolen, D. W. *Biochemistry* **1988**, *27*, 8063.
56. Handel, T. M.; Williams, S. A.; Menyhard, D.; DeGrado, W. F. *J. Am. Chem. Soc*. **1993**, *115*, 4457.
57. Wood, S. J.; MacKenzie, L; Maleeff, B.; Hurle, M. R.; Wetzel, R. *J. Biol. Chem*. **1996**, *271*, 4086.
58. Lai, Z.; Colón, W.; Kelly, J. W. *Biochemistry* **1996**, *35*, 6470.
59. Booth, D. R.; Sunde, M.; Bellotti, V.; Robinson, C. V.; Hutchinson, W. L.; Fraser, P. E.; Hawkins, P. N; Dobson, C. M.; Radford, S. E.; Blake, C. C. F.; Pepys; M. B. *Nature* **1997**, *385*, 787.
60. Mestel, R. *Nature* **1996**, *273*, 184.
61. Lundberg, K. M.; Stenland, C. J.; Cohen, F. E.; Prusiner; S. B.; Millhauser, G. L. *Chem. Biol*. **1997**, *4*, 345.
62. Rink, H. *Tetrahedron Lett*. **1987**, *28*, 3787.
63. Rivaille, P.; Gautron, J. P.; Castro, B.; Milhaud, G. *Tetrahedron* **1980**, *36*, 3413.
64. Yoshida, M.; Tatsumi, T.; Fujiwara, Y.; Iinuma, S.; Kimura, T.; Akaji, K.; Kiso, Y. *Chem. Pharm. Bull*. **1990**, *38*, 1551.
65. Tamamura, H.; Otaka, A.; Nakamura, J.; Okubo, K.; Koide, T.; Ikeda, K.; Fujii, N. *Tetrahedron Lett*. **1993**, *34*, 4931.